Superradiant Phase Transitions and the Standard Description of Circuit QED

Oliver Viehmann,[1] Jan von Delft,[1] and Florian Marquardt[2]

[1]*Physics Department, Arnold Sommerfeld Center for Theoretical Physics, and Center for NanoScience,
Ludwig-Maximilians-Universität, Theresienstraße 37, 80333 München, Germany*
[2]*Institut for Theoretical Physics, Universität Erlangen-Nürnberg, Staudtstraße 7, 91058 Erlangen, Germany*

We investigate the equilibrium behavior of a superconducting circuit QED system containing a large number of artificial atoms. It is shown that the currently accepted standard description of circuit QED via an effective model fails in an important aspect: it predicts the possibility of a superradiant phase transition, even though a full microscopic treatment reveals that a no-go theorem for such phase transitions known from cavity QED applies to circuit QED systems as well. We generalize the no-go theorem to the case of (artificial) atoms with many energy levels and thus make it more applicable for realistic cavity or circuit QED systems.

Recent years have seen rapid progress in fabrication and experimental control of superconducting circuit QED systems, in which a steadily increasing number of artificial atoms interact with microwaves [1–4]. These developments set the stage to study collective phenomena in circuit QED. An interesting question in that context is whether a system with many artificial atoms undergoes an equilibrium phase transition as the coupling of artificial atoms and electromagnetic field is increased (at zero temperature). Phase transitions of this type have been intensely discussed for cavity QED systems [5–10] and are known as superradiant phase transitions (SPTs) [6]. However, in cavity QED systems with electric dipole coupling their existence is doubted due to a no-go theorem [8]. Recently, it has been claimed that SPTs are possible in the closely related circuit QED systems with capacitive coupling [10–12]. This would imply that the no-go theorem of cavity QED does not apply and challenges the well-established analogy of circuit and cavity QED.

Here, we show in a full microscopic analysis that circuit QED systems are also subject to the no-go theorem. We argue that such an analysis is necessary since the standard description of circuit QED systems by an effective model (EM) is deficient in the regime considered here. A toy model is used to illustrate this failure of an EM. Finally, we close a possible loophole of the no-go theorem by generalizing it from two-level to multilevel (artificial) atoms. Thus, our work restores the analogy of circuit and cavity QED and rules out SPTs in these systems under realistic conditions that have not been covered before.

Dicke Hamiltonian in cavity and circuit QED.—Both circuit QED systems and cavity QED systems with N (artificial) atoms (Fig. 1) are often described by the Dicke Hamiltonian [13] ($\hbar = 1$)

$$\mathcal{H}_{\mathrm{D}} = \omega a^{\dagger} a + \frac{\Omega}{2} \sum_{k=1}^{N} \sigma_z^k + \frac{\lambda}{\sqrt{N}} \sum_{k=1}^{N} \sigma_x^k (a^{\dagger} + a)$$
$$+ \kappa (a^{\dagger} + a)^2. \tag{1}$$

The (artificial) atoms are treated as two-level systems with energy splitting Ω between ground state $|g\rangle_k = \binom{0}{1}_k$ and excited state $|e\rangle_k = \binom{1}{0}_k$ (σ_x^k, σ_z^k are Pauli matrices). In the case of circuit QED, we assume Cooper-pair boxes as artificial atoms, which justifies the two-level approximation. Our main results, though, hold for any charge-based artificial atoms (capacitive coupling) [14]. Further, $a^{\dagger}$ generates a photon of energy ω. Matter and field couple with a strength λ. The κ term, often neglected in other contexts, will become crucial below. In cavity QED, $\mathcal{H}_{\mathrm{D}}$ derives from minimal coupling of atoms and electromagnetic field. For an atom (n electrons) at a fixed position,

$$\mathcal{H}_{\mathrm{cav}}^0 = \sum_{i=1}^{n} \frac{[\mathbf{p}_i - e\mathbf{A}(\mathbf{r}_i)]^2}{2m} + V_{\mathrm{int}}(\mathbf{r}_1, \ldots, \mathbf{r}_n). \tag{2}$$

The $\mathbf{p}\mathbf{A}$ and $\mathbf{A}^2$ terms in the analog N-atom Hamiltonian yield the λ and κ term in $\mathcal{H}_{\mathrm{D}}$, respectively. In circuit QED, $\mathcal{H}_{\mathrm{D}}$ arises from a widely used EM for a charge-based artificial atom in a transmission line resonator [15],

$$\mathcal{H}_{\mathrm{cir}}^0 = 4E_C \sum_{\nu} (\nu - \bar{\nu})^2 |\nu\rangle\langle\nu| - \frac{E_J}{2} \sum_{\nu} (|\nu + 1\rangle\langle\nu| + \mathrm{H.c.}).$$

Here, ν counts the excess Cooper pairs on the island, E_J and $E_C = e^2/[2(C_G + C_J)]$ are the Josephson energy and
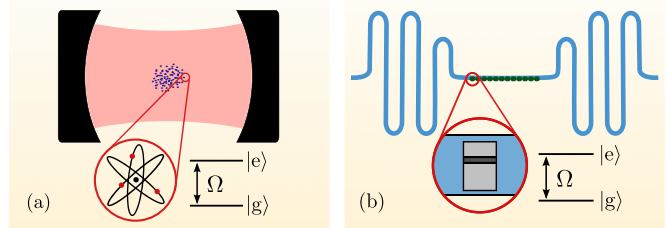

FIG. 1 (color online). Cavity QED system with N atoms (a) and circuit QED system with N Cooper-pair boxes as artificial atoms (b).

the charging energy of the Cooper-pair box, and C_G and C_J are the coupling capacitance and the capacitance of the Josephson junction. Moreover, $\bar{\nu} = C_G(V_G + \mathcal{V})/2e$, V_G is an external gate voltage and $\mathcal{V}$ the quantum voltage due to the electromagnetic field in the resonator. The Cooper-pair box is assumed to be at its degeneracy point [15]. As it is described by macroscopic quantities (like E_C) and only 1 degree of freedom (ν), $\mathcal{H}_0^{\text{cir}}$ is an EM for a Cooper-pair box in a transmission line. Starting either from $\mathcal{H}_{\text{cav}}^0$ or $\mathcal{H}_{\text{cir}}^0$, one obtains $\mathcal{H}_D$ using the following approximations: The N (artificial) atoms are identical, noninteracting two-level systems with ground and excited states $|g\rangle$ and $|e\rangle$ which are strongly localized compared to the wavelength of the single considered field mode [i.e., $\mathbf{A}(\mathbf{r}_i^k) \approx \mathbf{A} \equiv A_0 \boldsymbol{\epsilon}(a^\dagger + a)$, where $|\boldsymbol{\epsilon}| = 1$, and $\mathcal{V}(\mathbf{r}^k) \approx \mathcal{V} \equiv V_0(a^\dagger + a)$].

Superradiant phase transitions and no-go theorem.—In the limit $N \rightarrow \infty$, $\mathcal{H}_D$ undergoes a second order phase transition at a critical coupling strength [6–8]

$$\lambda_c^2 = \frac{\omega\Omega}{4}\left(1 + \frac{4\kappa}{\omega}\right). \tag{3}$$

This phase transition was discovered for $\mathcal{H}_D$ with $\kappa = 0$ and termed SPT [6]; see [9] for recent studies. At λ_c, the atoms polarize spontaneously, $\langle\sum_k \sigma_z^k\rangle/N \neq -1$, and a macroscopic photon occupation arises, $\langle a^\dagger a\rangle/N \neq 0$. A gapless excitation signals the critical point [Fig. 2(a)].

In cavity QED systems, however, λ_c cannot be reached if the κ term is not neglected [8]. That is because λ and κ are not independent of each other. Let us define a parameter α via $\kappa = \alpha\lambda^2/\Omega$. Then Eq. (3) becomes $\lambda_c^2(1 - \alpha) = \omega\Omega/4$, and criticality requires $\alpha < 1$. With $A_0 = 1/\sqrt{2\epsilon_0\omega V}$ (V is the volume of the cavity) one finds

$$\lambda_{\text{cav}} = \frac{\Omega|\boldsymbol{\epsilon}\cdot\mathbf{d}|}{\sqrt{2\epsilon_0\omega}}\sqrt{\frac{N}{V}}, \qquad \kappa_{\text{cav}} = \frac{n}{2\epsilon_0\omega}\frac{e^2}{2m}\frac{N}{V}, \tag{4}$$
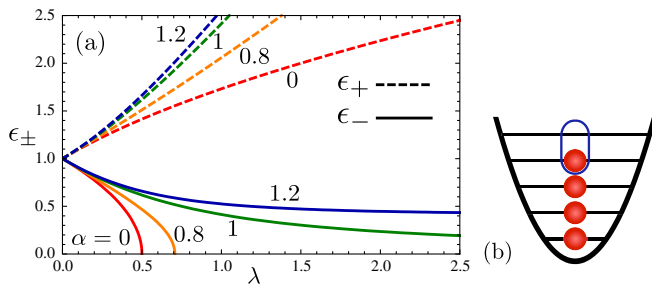

FIG. 2 (color online). (a) Excitation energies ϵ_+ and ϵ_- of the Dicke Hamiltonian $\mathcal{H}_D$ versus coupling λ (in units of $\omega = \Omega$), for $\alpha = \kappa\Omega/\lambda^2 = 0, 0.8, 1, 1.2$. For $\alpha = 0$, ϵ_- vanishes at $\lambda = 0.5$, thus signaling a SPT. Only $\alpha \geq 1$ is compatible with the TRK sum rule. For these α, $\epsilon_- \rightarrow \sqrt{1 - 1/\alpha}$ and remains finite for all λ. The excitations $\epsilon_\pm(\lambda)$ of $\mathcal{H}_{\text{tm}}$ correspond to $\alpha = 1$. (b) Toy model of an (artificial) atom. The oval line indicates the degree of freedom in the simplified effective model.

where $\mathbf{d} = \langle g|e\sum_{i=1}^n \mathbf{r}_i|e\rangle$ and $\alpha_{\text{cav}}\Omega|\boldsymbol{\epsilon}\cdot\mathbf{d}|^2 = ne^2/2m$. But the Thomas-Reiche-Kuhn sum rule (TRK) ([16], Sec. A)

$$\sum_l (E_l - E_g)|\boldsymbol{\epsilon}\cdot\langle g|e\sum_{i=1}^n \mathbf{r}_i|l\rangle|^2 = n\frac{e^2}{2m} \tag{5}$$

for the Hamiltonian $H^0 = \sum_{i=1}^n \mathbf{p}_i^2/2m + V_{\text{int}}(\mathbf{r}_1, \ldots, \mathbf{r}_n)$ of an uncoupled atom with spectrum $\{E_l, |l\rangle\}$ implies $\Omega|\boldsymbol{\epsilon}\cdot\mathbf{d}|^2 \leq ne^2/2m$, consequently $\alpha_{\text{cav}} \geq 1$. This is known as the no-go theorem for SPTs [8,10]. Notice that α_{cav} determines how strongly $\Omega|\boldsymbol{\epsilon}\cdot\mathbf{d}|^2$ exhausts the TRK. We remark that a direct dipole-dipole coupling between atoms (omitted here) can lead to a ferroelectric phase transition, which, however, occurs only at very high atomic densities [17].

Surprisingly, the no-go theorem was recently argued not to apply in circuit QED [10]. Indeed, the standard EM of circuit QED yields

$$\lambda_{\text{cir}} = \frac{eC_G}{C_G + C_J}\sqrt{\frac{\omega N}{Lc}}, \qquad \kappa_{\text{cir}} = \frac{C_G^2}{2(C_G + C_J)}\frac{\omega N}{Lc}, \tag{6}$$

where L denotes the length of the transmission line resonator, c its capacitance per unit length, and we have used $V_0 = (\omega/Lc)^{1/2}$ [15]. Here $\alpha_{\text{cir}} = E_J/4E_C < 1$ is easily possible [1]. According to this argument, a SPT should be observable in a circuit QED system.

Effective models and superradiant phase transitions.— The EM has proved to be a very successful description of circuit QED whose predictions have been confirmed in numerous experiments. However, the circuit QED setups operated so far contained only few artificial atoms. It is not obvious that an EM also provides a good description of circuit QED systems with $N \gg 1$ atoms and, thus, a proper starting point to study SPTs in circuit QED. We now present a toy model illustrating how an EM similar to the one in circuit QED can erroneously predict a SPT.

The toy model consists of N harmonic oscillator potentials with frequency Ω, each trapping n noninteracting fermions of mass m and charge e, which all couple to a bosonic mode with frequency ω [Fig. 2(b)].

This toy model can be viewed as a very simplified description of (artificial) atoms with n microscopic constituents inside a resonator. It is governed by the Hamiltonian

$$\mathcal{H}_{\text{tm}} = \omega a^\dagger a + \sum_{k=1}^N \sum_{i=1}^n \frac{(p_i^k - eA)^2}{2m} + \frac{m\Omega^2(x_i^k)^2}{2}, \tag{7}$$

where we assume again $A(x_i^k) \approx A = A_0(a^\dagger + a)$. Since A couples only to the center of mass coordinate of the kth oscillator, $\mathcal{H}_{\text{tm}}$ can be diagonalized ([16], Sec. B):

$$\mathcal{H}_{\text{tm}} = \epsilon_{\pm}\left(a_{\pm}^{\dagger} a_{\pm} + \frac{1}{2}\right) + \sum_{i=1}^{nN-1} \Omega\left(b_i^{\dagger} b_i + \frac{1}{2}\right),$$

$$2\epsilon_{\pm}^2(\lambda) = \omega^2 + 4\kappa\omega + \Omega^2$$

$$\pm \sqrt{(\omega^2 + 4\kappa\omega - \Omega^2)^2 + 16\lambda^2\omega\Omega}. \quad (8)$$

Here, $a_{\pm}^{\dagger}$ generate excitations that mix photon field with collective center of mass motion, the $b_i^{\dagger}$ excite the remaining degrees of freedom, $\lambda = A_0 \Omega d\sqrt{N}$ and $\kappa = \lambda^2/\Omega$. As $d = \langle n|ex|n-1\rangle = e\sqrt{n/2m\Omega}$, the TRK is exhausted. Note that $\epsilon_{\pm}(\lambda)$ are also the relevant excitation energies of $\mathcal{H}_{\text{D}}$ for $N \to \infty$, as can be shown using methods of Ref. [9] ([16], Sec. B), and demanding $\epsilon_- = 0$ yields Eq. (3). One sees that $\epsilon_{\pm}(\lambda)$ is real and nonzero for all λ and that the ground state energy is an analytic function of λ [Fig. 2(a)]. Hence, no phase transition is possible.

Let us now consider an EM for the toy model. Similar to the standard EM of circuit QED, we focus on the fermion with the highest energy in the kth harmonic oscillator and treat it as a two-level system with $|g_k\rangle = |n-1\rangle_k$ and $|e_k\rangle = |n\rangle_k$ [Fig. 2(b)]. Accounting only for one fermion per "atom," that is, expanding $\mathcal{H}_{\text{tm}}^{\text{EM}} = \omega a^{\dagger} a + \sum_{k=1}^{N} (p^k - eA)^2/2m + m\Omega^2(x^k)^2/2$ in the basis $\{|n-1\rangle_k, |n\rangle_k\}$, yields a Dicke Hamiltonian with $\lambda_{\text{EM}} = \lambda$ and $\kappa_{\text{EM}} = \kappa/n = Ne^2 A_0^2/2m$. Crucially, only λ_{EM} depends on n. This allows λ_{EM} to be increased at constant κ_{EM}; therefore, $\alpha_{\text{EM}} = 1/n$ can be <1 and a SPT is possible. This failure of the EM can be interpreted as follows. The relation $\lambda = \lambda_{\text{EM}} \propto d \propto \sqrt{n}$ reveals that the coupling of an "atom" to the bosonic mode is fully captured by the EM and grows with atom size n. However, in a proper description of the system, increasing the coupling by increasing n unavoidably also increases κ in proportion to n: all fermions of all atoms couple to the bosonic mode and each causes an A^2 term. This is lost in the EM with only 1 degree of freedom per atom. Interestingly, $\alpha_{\text{EM}} < 1$ only if $n > 1$, i.e., as long as the effective description actually neglects degrees of freedom.

Microscopic description of circuit QED.—This example suggests not to rely on the standard description for investigating SPTs in circuit QED. Although the dipole coupling of field and qubit states might be fully represented by λ_{cir}, κ_{cir} could still underestimate the A^2 terms of all charged particles in the Cooper-pair boxes. Instead, let us describe a circuit QED system with N artificial atoms by a minimal-coupling Hamiltonian that accounts for all microscopic degrees of freedom:

$$\mathcal{H}_{\text{mic}} = \omega a^{\dagger} a + \sum_{k=1}^{N} \sum_{i=1}^{n_k} \frac{(\mathbf{p}_i^k - q_i^k \mathbf{A})^2}{2m_i^k} + V_{\text{int}}(\mathbf{r}_1^k, \ldots, \mathbf{r}_{n_k}^k).$$

As we allow arbitrary charges q_i^k and masses m_i^k and an arbitrary interaction potential V_{int} of the n_k constituents of the kth artificial atom, $\mathcal{H}_{\text{mic}}$ most generally captures the coupling of N arbitrary (but mutually noninteracting)

objects to the electromagnetic field. We subject it to the same approximations that led from $\mathcal{H}_{\text{cir}}^0$, the EM of circuit QED, to $\mathcal{H}_{\text{D}}$. For identical artificial atoms $\{n_k, q_i^k, m_i^k\} \to \{n, q_i, m_i\}$. The Hamiltonian of an uncoupled artificial atom then reads $H_{\text{mic}}^0 = \sum_{i=1}^{n} \mathbf{p}_i^2/2m_i + V_{\text{int}}(\mathbf{r}_1, \ldots, \mathbf{r}_n)$. Its qubit states $|g\rangle$ and $|e\rangle$, which in the standard EM are superpositions of the charge states $|\nu\rangle$, are among the eigenstates $\{|l\rangle\}$ of H_{mic}^0. Expanding $\mathcal{H}_{\text{mic}}$ in the $\{|g\rangle_k, |e\rangle_k\}$ basis and taking $\mathbf{A}(\mathbf{r}_i^k) \approx \mathbf{A}$ gives the Dicke Hamiltonian $\mathcal{H}_{\text{D}}$ with parameters generalizing those of cavity QED [Eq. (4)],

$$\lambda_{\text{cir}}^{\text{mic}} = \frac{\Omega|\boldsymbol{\epsilon} \cdot \mathbf{d}|}{\sqrt{2\epsilon_0\omega}}\sqrt{\frac{N}{V}}, \qquad \kappa_{\text{cir}}^{\text{mic}} = \frac{1}{2\epsilon_0\omega}\left(\sum_{i=1}^{n} \frac{q_i^2}{2m_i}\right)\frac{N}{V}, \quad (9)$$

where $\mathbf{d} = \langle g|\sum_{i=1}^{n} q_i \mathbf{r}_i|e\rangle$. This microscopic description of circuit QED facilitates the same line of argument which in Ref. [8] allowed the conclusion that there is no SPT in cavity QED: Criticality [Eq. (3)] requires $\Omega|\boldsymbol{\epsilon} \cdot \mathbf{d}|^2 > \sum_{i=1}^{n} q_i^2/2m_i$, which is ruled out by TRK for H_{mic}^0,

$$\sum_l (E_l - E_g)|\boldsymbol{\epsilon} \cdot \langle g|\sum_{i=1}^{n} q_i \mathbf{r}_i|l\rangle|^2 = \sum_{i=1}^{n} \frac{q_i^2}{2m_i}. \quad (10)$$

Hence, the no-go theorem of cavity QED applies to circuit QED as well. This result confirms the analogy of cavity and circuit QED also with respect to SPTs. It has been obtained under the same approximations that led from the standard description of circuit QED, $\mathcal{H}_{\text{cir}}^0$, to $\mathcal{H}_{\text{D}}$ with λ_{cir} and κ_{cir}. The discrepancy of the predictions of the microscopic and the standard description of circuit QED thus shows the limitations of the validity of the latter. This might be important for future circuit QED architectures with many artificial atoms in general, even for applications not related to SPTs. We emphasize, though, that our conclusion neither forbids SPTs in circuit QED systems with inductively coupling flux qubits [18] nor is it at odds with the great success of the standard description for few-atom systems: there, the deficiency of κ_{cir} does not manifest itself qualitatively as the κ term in $\mathcal{H}_{\text{D}}$ mimics slightly renormalized system parameters $\tilde{\omega}$ and $\tilde{\lambda}$.

Possible loophole in the no-go theorem.—Although the two-level approximation for the anharmonic spectrum of (artificial) atoms is well justified in many cases, one might argue that higher levels should be taken into account in this context. Indeed, a SPT does not require $\Omega \approx \omega$, and thereby does not single out a particular atomic transition.

For a more profound reason for dropping the two-level assumption, consider the elementary question of how the presence of N mutually noninteracting atoms shifts a resonator's frequency ω. This situation is described by $\mathcal{H}_{\text{mic}}$. It can be rewritten as $\mathcal{H}_{\text{mic}} = \omega a^{\dagger} a + \sum_{k=1}^{N} (H_{\text{mic}}^k + \mathcal{H}_{pA}^k + \mathcal{H}_{A^2}^k)$, where $\mathcal{H}_{pA}^k$ and $\mathcal{H}_{A^2}^k$ are the $\mathbf{p}\mathbf{A}$ and A^2 terms due to the kth atom ([16], Sec. C). Let us perturbatively calculate the frequency shift $\delta\omega = \delta\omega_{pA} + \delta\omega_{A^2}$ caused by $\sum \mathcal{H}_{pA}^k$ and $\sum \mathcal{H}_{A^2}^k$ ([16], Sec. C). To this end,

take $\omega \ll \Omega_m^k$ for all m, k, where Ω_m^k is the mth excitation energy of H_{mic}^k. Remarkably, it turns out ([16], Sec. C) that $\delta\omega_{pA}$ (< 0) and $\delta\omega_{A^2}$ (> 0) cancel almost exactly due to the TRK. The total frequency shift is small, $\delta\omega \sim (\omega/\Omega_m^k)^2$. As a SPT equates to $\delta\omega = -\omega$, the significance of both $\mathbf{pA}$ and $\mathbf{A}^2$ terms for its existence becomes clear. The $\mathbf{pA}$ terms cause a strong negative shift and favor a SPT, the $\mathbf{A}^2$ terms do the opposite. This means, most crucially, that one must not unequally truncate $\mathbf{pA}$ and $\mathbf{A}^2$ terms for assessing the possibility of a SPT by an approximate Hamiltonian. Dropping the $\mathbf{A}^2$ terms in $\mathcal{H}_D$ ($\kappa = 0$) leads to the prediction of a SPT. In contrast, $\mathcal{H}_D$ with $\kappa \neq 0$ fully incorporates the $\mathbf{A}^2$ terms of $\mathcal{H}_{\text{mic}}$. But, due to the two-level approximation, it has only one matrix element of the $\mathbf{pA}$ terms per atom, thereby possibly underestimating the tendency towards a SPT. To exclude SPTs in cavity and circuit QED, a generalization of the no-go theorem to (artificial) atoms with more than two energy levels is necessary.

Generalized no-go theorem.—Let us consider $N \to \infty$ identical atoms coupled to a field mode with frequency ω. The atomic Hamiltonians H_{mic}^k may have an arbitrary spectrum $\{\Omega_l, |l\rangle_k = |l\rangle_k\}$, with $\Omega_0 = 0$ and μ excited states (Fig. 3).

With $d_{l,l'} = \boldsymbol{\epsilon} \cdot \langle l | \sum_{i=1}^n q_i \mathbf{r}_i | l' \rangle$, the full Hamiltonian of the system reads

$$\mathcal{H}_{\text{mic}} = \omega a^\dagger a + \kappa(a^\dagger + a)^2 + \sum_{k=1}^N \sum_{l,l'=0}^\mu (\Omega_l \delta_{l,l'} |l\rangle_k \langle l_k|$$
$$+ iA_0(\Omega_{l'} - \Omega_l)d_{l,l'}(a^\dagger + a)|l\rangle_k \langle l'_k|). \quad (11)$$

We now follow a strategy similar to that of Refs. [9]: We derive a generalized Dicke Hamiltonian $\mathcal{H}_{\text{GD}}$ having the same low-energy spectrum as $\mathcal{H}_{\text{mic}}$ for a small density of atoms, $N/V \simeq 0$, using $A_0 \propto V^{-1/2}$ as small parameter. We then check whether $\mathcal{H}_{\text{GD}}$ has a gapless excitation if the density is increased, which would signal a SPT and mark the breakdown of the analogy of $\mathcal{H}_{\text{GD}}$ and $\mathcal{H}_{\text{mic}}$.

Expanding the eigenstates and eigenenergies of $\mathcal{H}_{\text{mic}}$ as $|\mathcal{E}\rangle \propto \sum_{s=0}^\infty A_0^s |\mathcal{E}_s\rangle$ and $\mathcal{E} \propto \sum_{ss'} A_0^{s+s'} \langle \mathcal{E}_s | \mathcal{H}_{\text{mic}} | \mathcal{E}_{s'} \rangle$, we note that contributions from all $d_{l\neq0,l'\neq0}$ terms may be neglected: they are smaller than those retained by a factor of at least one power of A_0 (for $s + s' > 1$) or $\xi/N \ll 1$ (for $s + s' \leq 1$), where $\xi = \sum_k \sum_{l>0} |\langle l_k | \mathcal{E}_0 \rangle|^2$ is the number of atomic excitations in $|\mathcal{E}_0\rangle$, which is $\ll N$ for
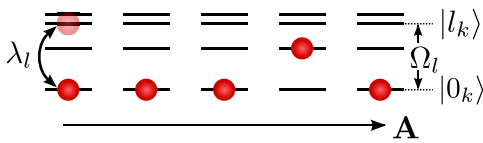

FIG. 3 (color online). Situation of the generalized no-go theorem. Many multilevel (artificial) atoms couple to the photon field. Transitions between excited atomic states are irrelevant for the low-energy spectrum of the system.

low-lying eigenstates ([16], Sec. D). We thus define $\mathcal{H}_{\text{GD}}$ by setting $d_{l\neq0,l'\neq0} \to 0$ in $\mathcal{H}_{\text{mic}}$. Up to a constant, we find ([16], Sec. D)

$$\mathcal{H}_{\text{GD}} = \tilde{\omega} a^\dagger a + \sum_{l=1}^\mu \Omega_l b_l^\dagger b_l + \sum_{l=1}^\mu \tilde{\lambda}_l (b_l^\dagger + b_l)(a^\dagger + a),$$
$$(12)$$

by introducing $b_l^\dagger = \frac{1}{\sqrt{N}} \sum_{k=1}^N |l_k\rangle\langle 0_k|$ as collective excitation, omitting the energy of the "dark" collective excitations ([16], Sec. D), and removing the κ term by a Bogolyubov transformation yielding $\omega \to \tilde{\omega} = \sqrt{\omega^2 + 4\kappa\omega}$ and $\lambda_l \to \tilde{\lambda}_l = \sqrt{\frac{\omega}{\tilde{\omega}}}\lambda_l$, with $\lambda_l = A_0 \Omega_l |d_{0,l}| \sqrt{N}$. For dilute excitations, the b_l are bosonic, $[b_l, b_{l'}^\dagger] = \delta_{l,l'}$ [19]. The system undergoes a SPT if an eigenfrequency ϵ_i of $\mathcal{H}_{\text{GD}}$ can be pushed to zero by increasing the couplings λ_l. We cannot calculate the ϵ_i's explicitly, but we will show that the assumption $\epsilon_i = 0$ contradicts the TRK. An ϵ_i solves the characteristic equation ([16], Sec. D)

$$\left(\prod_{l'=1}^\mu (\Omega_{l'}^2 - \epsilon^2) \right)\left((\tilde{\omega}^2 - \epsilon^2) - 4\tilde{\omega} \sum_{l=1}^\mu \frac{\Omega_l \tilde{\lambda}_l^2}{\Omega_l^2 - \epsilon^2} \right) = 0. \quad (13)$$

If ϵ_i were zero, this would imply

$$\frac{\omega}{4NA_0^2} = \sum_{l=1}^\mu \Omega_l |d_{0l}|^2 - \sum_{i=1}^n \frac{q_i^2}{2m_i} \quad (14)$$

and contradict the TRK for H_{mic}^0 [Eq. (10)], which ensures that the right-hand side is negative even if the entire atomic spectrum is incorporated. This result is irrespective of the details of the atomic spectra. Note that for $\kappa = 0$, the negative term on the right-hand side of Eq. (14) vanishes, and one recovers the SPT for critical couplings λ_{lc} with $\sum_{l=1}^\mu \lambda_{lc}^2/\Omega_l = \omega/4$. This resembles Eq. (3) with $\kappa = 0$.

Experimental evidence for our conclusions could be gained by probing the shifted resonator frequency of a suitable circuit QED system. Consider a sample containing N artificial atoms with $\lambda/\sqrt{N} = 2\pi \times 120$ MHz and $\Omega/2\pi = \omega/2\pi = 3$ GHz. If $\alpha_{\text{cir}} = E_J/4E_C = 0.1$, as predicted by the standard theory, there should be signatures of criticality for $N = 174$ [according to Eq. (3)], and the resonator frequency should be close to zero. But even if we assume $\alpha = 1$, the minimal value compatible with the TRK (that corresponds to ideal two-level atoms), we find the lowest excitation ϵ_- to be still at $\epsilon_- \approx 2\pi \times 2$ GHz. We have verified that these phenomena are insensitive to small fluctuations of the atomic parameters ([16], Sec. E; see also [18]) and hence experimentally observable.

[1] A. Wallraff *et al.*, Nature (London) **431**, 162 (2004).

[2] J. M. Fink *et al.*, Phys. Rev. Lett. **103**, 083601 (2009).

[3] M. Neeley *et al.*, Nature (London) **467**, 570 (2010).

[4] L. DiCarlo *et al.*, Nature (London) **467**, 574 (2010).

[5] J. M. Raimond, M. Brune, and S. Haroche, Rev. Mod. Phys. **73**, 565 (2001).

[6] K. Hepp and E. H. Lieb, Ann. Phys. (N.Y.) **76**, 360 (1973).

[7] Y. K. Wang and F. T. Hioe, Phys. Rev. A **7**, 831 (1973).

[8] K. Rzążewski, K. Wódkiewicz, and W. Żakowicz, Phys. Rev. Lett. **35**, 432 (1975).

[9] C. Emary and T. Brandes, Phys. Rev. Lett. **90**, 044101 (2003); C. Emary and T. Brandes, Phys. Rev. E **67**, 066203 (2003).

[10] P. Nataf and C. Ciuti, Nature Commun. 1 (2010) 72.

[11] G. Chen, Z. Chen, and J. Liang, Phys. Rev. A **76**, 055803 (2007).

[12] N. Lambert *et al.*, Phys. Rev. B **80**, 165308 (2009).

[13] R. H. Dicke, Phys. Rev. **93**, 99 (1954).

[14] J. Clarke and F. Wilhelm, Nature (London) **453**, 1031 (2008).

[15] A. Blais *et al.*, Phys. Rev. A **69**, 062320 (2004).

[16] See Supplemental Material at http://link.aps.org/supplemental/10.1103/PhysRevLett.107.113602 for further explanation and details of the calculations.

[17] J. Keeling, J. Phys. Condens. Matter **19**, 295213 (2007).

[18] P. Nataf and C. Ciuti, Phys. Rev. Lett. **104**, 023601 (2010).

[19] J. J. Hopfield, Phys. Rev. **112**, 1555 (1958).

EPAPS: Supplementary Information for "Superradiant Phase Transitions and the Standard Description of Circuit QED"

Oliver Viehmann[1], Jan von Delft[1], and Florian Marquardt[2]

[1] *Physics Department, Arnold Sommerfeld Center for Theoretical Physics, and Center for NanoScience, Ludwig-Maximilians-Universität, Theresienstrasse 37, 80333 Munich, Germany*
[2] *Institut for Theoretical Physics, Universität Erlangen-Nürnberg, Staudtstraße 7, 91058 Erlangen, Germany*

We provide intermediate steps for the derivation of some important statements and equations of the main text (Secs. A-D). Furthermore, we discuss the influence of disorder in the parameters of artificial atoms on a possible experimental verification of our results (Sec. E). For clarity, formulas contained in the main text are typeset in blue.

A. Thomas-Reiche-Kuhn sum rule. We derive the TRK [1] for the Hamiltonian

$$H_{\text{mic}}^0 = \sum_{i=1}^n \frac{\mathbf{p}_i^2}{2m_i} + V_{\text{int}}(\mathbf{r}_1, \ldots, \mathbf{r}_n), \tag{S1}$$

yielding Eq. (9) of the main text; Eq. (4) follows as a special case. The derivation of the TRK is based upon the identities

$$\sum_{i=1}^n \frac{q_i^2}{2m_i} = -i\Big[\boldsymbol{\epsilon} \cdot \sum_{i=1}^n q_i\mathbf{r}_i\,,\boldsymbol{\epsilon} \cdot \sum_{i'=1}^n \frac{q_{i'}\mathbf{p}_{i'}}{2m_{i'}}\Big], \qquad \sum_{i=1}^n \frac{q_i\mathbf{p}_i}{m_i} = i\Big[H_{\text{mic}}^0, \sum_{i=1}^n q_i\mathbf{r}_i\Big], \tag{S2}$$

for a real unit vector $\boldsymbol{\epsilon}$. We denote the eigenspectrum of H_{mic}^0 by $\{E_l, |l\rangle\}$. It comprises a ground state $|g\rangle$ of energy E_g. The TRK follows by combining the commutators of Eqs. (S2):

$$\sum_{i=1}^n \frac{q_i^2}{2m_i} = \langle g|\Big[\boldsymbol{\epsilon} \cdot \sum_{i=1}^n q_i\mathbf{r}_i\,,\frac{\boldsymbol{\epsilon}}{2} \cdot \Big[H_{\text{mic}}^0, \sum_{i'=1}^n q_{i'}\mathbf{r}_{i'}\Big]\Big]|g\rangle \tag{S3a}$$

$$= \sum_l (E_l - E_g)|\boldsymbol{\epsilon} \cdot \langle g| \sum_{i=1}^n q_i\mathbf{r}_i|l\rangle|^2. \tag{S3b}$$

B. Diagonalization of $\mathcal{H}_\mathrm{D}$ and $\mathcal{H}_\mathrm{tm}$. It is demonstrated that the diagonalization of both the Dicke Hamiltonian $\mathcal{H}_\mathrm{D}$ for $N \to \infty$ and the Hamiltonian $\mathcal{H}_\mathrm{tm}$ describing the toy model can be reduced to the diagonalization of special cases of $\mathcal{H}_\mathrm{GD}$, which appears in the context of the generalized no-go theorem. The characteristic equation of $\mathcal{H}_\mathrm{GD}$, that will be derived in Sec. D of these supplementary notes, is solvable for the special cases and yields the diagonal forms of $\mathcal{H}_\mathrm{D}$ and $\mathcal{H}_\mathrm{tm}$.

Diagonalization of $\mathcal{H}_\mathrm{D}$. First, we focus on the Dicke Hamiltonian

$$\mathcal{H}_\mathrm{D} = \omega a^\dagger a + \frac{\Omega}{2}\sum_{k=1}^{N}\sigma_z^k + \frac{\lambda}{\sqrt{N}}\sum_{k=1}^{N}\sigma_x^k(a^\dagger + a) + \kappa(a + a^\dagger)^2 \tag{S4a}$$

$$= \tilde{\omega}a^\dagger a + \frac{\Omega}{2}\sum_{k=1}^{N}\sigma_z^k + \frac{\tilde{\lambda}}{\sqrt{N}}\sum_{k=1}^{N}\sigma_x^k(a^\dagger + a) + C \tag{S4b}$$

with $\tilde{\omega} = \sqrt{\omega^2 + 4\kappa\omega}$, $\tilde{\lambda} = \sqrt{\omega/\tilde{\omega}}\lambda$, and $C = (\tilde{\omega} - \omega)/2$. The Hamiltonian (S4b) was diagonalized by means of a Holstein-Primakoff transformation in Refs. [2]. We employ here a closely related approach developed in [3], which is more convenient for a generalization beyond the two-level approximation and was also used in the derivation of $\mathcal{H}_\mathrm{GD}$. We drop C, set the energy of the atomic ground states to zero, introduce the operators

$$a_k^\dagger = |e_k\rangle\langle g_k|, \qquad b_{q_j}^\dagger = \frac{1}{\sqrt{N}}\sum_{k=1}^{N}e^{iq_jk}|e_k\rangle\langle g_k|, \tag{S5}$$

where $q_j = 2\pi(j/N)$ and $j \in \{0, 1, \ldots, N-1\}$, and obtain for $N \to \infty$

$$\mathcal{H}_\mathrm{D}' = \tilde{\omega}a^\dagger a + \Omega\sum_{k=1}^{N}a_k^\dagger a_k + \tilde{\lambda}(b_{q_0}^\dagger + b_{q_0})(a^\dagger + a) \tag{S6a}$$

$$= \tilde{\omega}a^\dagger a + \Omega\sum_{j=0}^{N-1}b_{q_j}^\dagger b_{q_j} + \tilde{\lambda}(b_{q_0}^\dagger + b_{q_0})(a^\dagger + a). \tag{S6b}$$

In the limit of dilute excitations, that is applicable as long as the excitation energies of the system are finite, the b_{q_j} obey bosonic commutation relations. Note that only the $j = 0$ collective mode couples to the radiation field. The $j \neq 0$ modes are 'dark' and will be omitted in the following. We write b instead of b_{q_0} and arrive at

$$\mathcal{H}_\mathrm{D}'' = \tilde{\omega}a^\dagger a + \Omega b^\dagger b + \tilde{\lambda}(b^\dagger + b)(a^\dagger + a), \tag{S7}$$

which corresponds to $\mathcal{H}_\mathrm{GD}$ (Eqs. (11) and (S28)) with $\mu = 1$. Later we will derive a characteristic equation for the eigenfrequencies of $\mathcal{H}_\mathrm{GD}$ (Eqs. (12) and (S32b)). For $\mu = 1$ this equation has the solutions

$$2\epsilon_\pm^2 = \omega^2 + 4\kappa\omega + \Omega^2 \pm \sqrt{(\omega^2 + 4\kappa\omega - \Omega^2)^2 + 16\lambda^2\omega\Omega}. \tag{S8}$$

Diagonalization of $\mathcal{H}_{\mathrm{tm}}$. Now we consider $\mathcal{H}_{\mathrm{tm}}$ (Eq. (6)). The coupling of the electromagnetic field and a single harmonic oscillator 'atom' is described by

$$\mathcal{H}_{\mathrm{tm}}^0 = \sum_{i=1}^n \frac{(p_i - eA)^2}{2m} + \frac{m\Omega^2 x_i^2}{2}. \tag{S9}$$

Note that we drop the index k numbering the atoms in $\mathcal{H}_{\mathrm{tm}}$ for a moment. As usual, we assume $\mathbf{A}(\mathbf{r}) \approx \mathbf{A} = A_0(a^\dagger + a)$ in the region where the atoms are located. It is convenient to make the canonical transformation $\tilde{x}_i = -p_i/(m\Omega)$ and $\tilde{p}_i = m\Omega x_i$. This yields

$$\mathcal{H}_{\mathrm{tm}}^0 = \sum_{i=1}^n \left(\frac{p_i^2}{2m} + \frac{m\Omega^2 x_i^2}{2} \right) + eA_0\Omega(a^\dagger + a) \sum_{i=1}^n x_i + \frac{ne^2 A_0^2}{2m}(a^\dagger + a)^2, \tag{S10}$$

where we have written x_i and p_i instead of $\tilde{x}_i$ and $\tilde{p}_i$ to keep notation simple. Successively introducing relative and center-of-mass coordinates, $\{x_1, p_1, x_2, p_2\} \to \{\tilde{x}_1, \tilde{p}_1, X_1, P_1\}$, $\{X_1, P_1, x_3, p_3\} \to \{\tilde{x}_2, \tilde{p}_2, X_2, P_2\}$, ..., leads to

$$\mathcal{H}_{\mathrm{tm}}^0 = \sum_{i=1}^{n-1} \left(\frac{\tilde{p}_i^2}{2\mu_i} + \frac{\mu_i \Omega^2 \tilde{x}_i^2}{2} \right) + \frac{\tilde{P}^2}{2M} + \frac{M\Omega^2 X^2}{2} + eA_0\Omega(a^\dagger + a)nX + \frac{ne^2 A_0^2}{2m}(a^\dagger + a)^2. \tag{S11}$$

Here, $X = X_n = \frac{1}{n} \sum_{j=1}^n x_j$ and $P = P_n = \sum_{j=1}^n p_j$ are the center-of-mass coordinates of all particles in the harmonic oscillator atom, and $M = nm$. The relative coordinates are given by $\tilde{x}_i = (1/i \sum_{j=1}^i x_j) - x_{i+1}$ and $\tilde{p}_i = 1/(i+1)(\sum_{j=1}^i p_j - ip_{j+1})$, and $\mu_i = mi/(i+1)$. Note that the electromagnetic field couples only to the center of mass. With this preliminary work done, one can write the full Hamiltonian as

$$\mathcal{H}_{\mathrm{tm}} = \tilde{\omega} a^\dagger a + \Omega \sum_{k=1}^N c_k^\dagger c_k + \tilde{\gamma} \sum_{k=1}^N (c_k^\dagger + c_k)(a^\dagger + a) + \Omega \sum_{i=1}^{N(n-1)} \left(b_i^\dagger b_i + \frac{1}{2} \right) + C'. \tag{S12}$$

The operator $c_k^\dagger$ excites the center-of-mass degree of freedom of the kth atom, and the generators for the $N(n-1)$ relative coordinates are denoted by $b_i^\dagger$. We have introduced

$$\gamma = eA_0 \sqrt{\frac{n\Omega}{2m}}, \qquad \kappa = nN \frac{e^2 A_0^2}{2m}, \tag{S13}$$

and removed the κ-term by means of $\tilde{\omega} = \sqrt{\omega^2 + 4\kappa\omega}$ and $\tilde{\gamma} = \sqrt{\omega/\tilde{\omega}}\gamma$ as before ($C' = (\tilde{\omega} - \omega + N\Omega)/2$). The first three terms are again a special case of $\mathcal{H}_{\mathrm{GD}}$ with $\Omega_l = \Omega$ and $\tilde{\lambda}_l = \tilde{\gamma}$ for all l, and $\mu = N$. Hence, their eigenvalues follow from the roots of the characteristic equation for $\mathcal{H}_{\mathrm{GD}}$ (Eq. (S32b)), simplified by the present conditions. They can be explicitly calculated and are the frequencies of the normal modes of field and center-of-mass coordinates. We find $N - 1$ eigenfrequencies being equal to Ω and represent the generators of the corresponding collective excitations also by $b_i^\dagger$. Only two eigenfrequencies $\epsilon_\pm$ are nondegenerate,

$$2\epsilon_\pm^2 = \omega^2 + 4\kappa\omega + \Omega^2 \pm \sqrt{(\omega^2 + 4\kappa\omega - \Omega^2)^2 + 16N\gamma^2\omega\Omega} \tag{S14a}$$

$$= \omega^2 + 4\kappa\omega + \Omega^2 \pm \sqrt{(\omega^2 + 4\kappa\omega - \Omega^2)^2 + 16\lambda^2\omega\Omega}. \tag{S14b}$$

We have defined $\lambda = \sqrt{N}\gamma$. Since the dipole moment d of the transition from the ground state of an atom to its first excited state is given by $d = \langle n|ex|n-1\rangle = e\sqrt{n/2m\Omega}$, we can rewrite $\lambda = A_0\Omega d\sqrt{N}$ and $\kappa = \lambda^2/\Omega$. Denoting the generators of the $\epsilon_\pm$-modes by $a_\pm$, we arrive at

$$\mathcal{H}_{\mathrm{tm}} = \epsilon_\pm(a_\pm^\dagger a_\pm + \frac{1}{2}) + \sum_{i=1}^{nN-1} \Omega(b_i^\dagger b_i + \frac{1}{2}) - \frac{\omega}{2}. \tag{S15}$$

C. Shift of the resonator frequency due to the pA- and A^2-terms. Consider a system of N mutually noninteracting objects (e.g. atoms) with Hamiltonians

$$H_{\mathrm{mic}}^k = \sum_{i=1}^{n_k} \frac{(\mathbf{p}_i^k)^2}{2m_i^k} + V_{\mathrm{int}}(\mathbf{r}_1^k, \ldots, \mathbf{r}_{n_k}^k) \tag{S16}$$

coupled to a field mode of frequency ω. It is described by

$$\mathcal{H}_{\mathrm{mic}} = \omega a^\dagger a + \sum_{k=1}^{N} \left(H_{\mathrm{mic}}^k + \mathcal{H}_{pA}^k + \mathcal{H}_{A^2}^k\right), \tag{S17}$$

where $H_{\mathrm{mic}}^k = \sum_{i=1}^{n_k}(\mathbf{p}_i^k)^2/2m_i^k + V_{\mathrm{int}}(\mathbf{r}_1^k, \ldots, \mathbf{r}_{n_k}^k)$, $\mathcal{H}_{pA}^k = -\sum_{i=1}^{n_k} q_i^k \mathbf{A}\mathbf{p}_i^k/m_i^k$, and $\mathcal{H}_{A^2}^k = \sum_{i=1}^{n_k}(q_i^k)^2\mathbf{A}^2/2m_i^k$. We denote the eigenspectrum of H_{mic}^k by $\{E_{m_k}^k, |m_k\rangle_k\}$ and the photon states by $|l\rangle$ and calculate the shifts $\delta\omega_{pA}$ and $\delta\omega_{A^2}$ of the resonator frequency due to $\sum \mathcal{H}_{pA}^k$ and $\sum \mathcal{H}_{A^2}^k$ using the first nonzero terms in a perturbation series for the energy of $|0, \ldots, 0, l\rangle$. We take $\omega \ll (E_{m_k}^k - E_0^k) =: \Omega_{m_k}^k$ for $m_k \neq 0$ and $\mathbf{A}(\mathbf{r}_i^k) \approx \mathbf{A}$. With $\mathbf{d}_{m_k,0}^k = {}_k\langle m_k| \sum_{i=1}^{n_k} q_i^k \mathbf{r}_i^k|0\rangle_k$, we find for the jth terms ΔE_{pA}^j and $\Delta E_{A^2}^j$ in the perturbation series for the perturbations $\sum \mathcal{H}_{pA}^k$ and $\sum \mathcal{H}_{A^2}^k$

$$\Delta E_{pA}^1 = 0 \tag{S18a}$$

$$\Delta E_{pA}^2 = -A_0^2 \sum_{k=1}^{N} \sum_{m_k \neq 0} \Omega_{m_k}^k |\boldsymbol{\epsilon} \cdot \mathbf{d}_{m_k,0}^k|^2 \left(\frac{(l+1)}{1+\frac{\omega}{\Omega_{m_k}^k}} + \frac{l}{1-\frac{\omega}{\Omega_{m_k}^k}}\right) \tag{S18b}$$

$$\approx -A_0^2 \sum_{k=1}^{N} \sum_{m_k \neq 0} \Omega_{m_k}^k |\boldsymbol{\epsilon} \cdot \mathbf{d}_{m_k,0}^k|^2 \left((2l+1) - \left(\frac{\omega}{\Omega_{m_k}^k}\right) + (2l+1)\left(\frac{\omega}{\Omega_{m_k}^k}\right)^2\right) \tag{S18c}$$

$$\Delta E_{A^2}^1 = A_0^2(2l+1) \sum_{k=1}^{N} \sum_{i=1}^{n_k} \frac{(q_i^k)^2}{2m_i^k} \tag{S18d}$$

Therefore,

$$\delta\omega_{pA} = -2A_0^2 \sum_{k=1}^{N} \sum_{m_k \neq 0} \Omega_{m_k}^k |\boldsymbol{\epsilon} \cdot \mathbf{d}_{m_k,0}^k|^2 \left(1 + \frac{\omega^2}{(\Omega_{m_k}^k)^2}\right) \tag{S19a}$$

$$\delta\omega_{A^2} = 2A_0^2 \sum_{k=1}^{N} \sum_{i=1}^{n_k} \frac{(q_i^k)^2}{2m_i^k}. \tag{S19b}$$
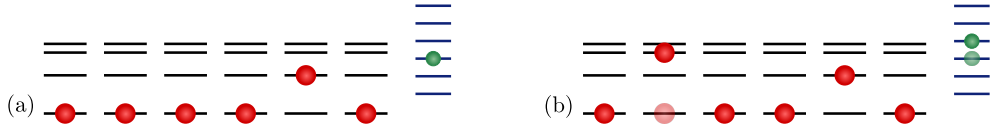
4

Figure S1: Situation of the generalized no-go theorem. Atomic spectra are drawn black, eigenenergies of the free electromagnetic field blue. (a) Structure of a low-energy state $|\mathcal{E}_0\rangle$ of the uncoupled system. For $N \to \infty$, the numbers of excited atoms ξ and of photons χ in $|\mathcal{E}_0\rangle$ are small compared to N, $\xi \ll N$ and $\chi \ll N$. (b) Structure of a component of $\mathcal{E}_1$. The coupling has induced one atomic transition and created or annihilated one photon (shown is an excitation of the second atom and the creation of a photon). The state $|\mathcal{E}_1\rangle$ is the sum of all such states. Their amplitude in the eigenstate of the coupled system is smaller than the amplitude of $|\mathcal{E}_0\rangle$ by a factor $\propto A_0 \propto V^{-1/2}$. In general, $|\mathcal{E}_s\rangle$ represents the sum over all states obtained from $|\mathcal{E}_0\rangle$ via s atomic transitions and s creations or annihilations of a photon. They contribute to the eigenstate of the coupled system by an amplitude $\propto A_0^s$.

The **pA**-terms cause a negative and the **A^2**-terms a positive frequency shift. Note that $\delta\omega_{pA}$ and $\delta\omega_{A^2}$ almost cancel due to the TRK (applied for each k). The resulting total frequency shift $\delta\omega = \delta\omega_{pA} + \delta\omega_{A^2}$ is suppressed by $\sim (\omega/\Omega_{m_k}^k)^2$ as compared with $\delta\omega_{pA}$ and $\delta\omega_{A^2}$.

D. The generalized Dicke Hamiltonian $\mathcal{H}_{\mathrm{GD}}$. In this section, we derive the Hamiltonian $\mathcal{H}_{\mathrm{GD}}$ (Eq. (11)) from $\mathcal{H}_{\mathrm{mic}}$ (in the form of Eq. (10)) for $N \to \infty$ and show how to obtain and evaluate its characteristic equation.

According to our strategy formulated in the main text, we start from low atomic densities and expand the eigenstates $|\mathcal{E}\rangle$ of $\mathcal{H}_{\mathrm{mic}}$ in powers of $A_0 \propto V^{-1/2}$,

$$|\mathcal{E}\rangle \propto \sum_{s=0}^{\infty} A_0^s |\mathcal{E}_s\rangle, \tag{S20}$$

where $|\mathcal{E}_s\rangle$ stands for a sum over components that each describe s transitions from $|\mathcal{E}_0\rangle$ both in its atomic and in its photonic part and hence has weight $\propto A_0^s$ (Fig. S1). The corresponding eigenenergies can be written as $\mathcal{E} \propto \sum_{ss'} A_0^{s+s'} \langle \mathcal{E}_s | \mathcal{H}_{\mathrm{mic}} | \mathcal{E}_{s'} \rangle$. We are interested only in the low-energy spectrum of $\mathcal{H}_{\mathrm{mic}}$. Thus, we assume that the number of atomic excitations $\xi = \sum_k \sum_{l>0} |\langle l_k | \mathcal{E}_0 \rangle|^2$ and the number of photons $\chi = \langle \mathcal{E}_0 | a^\dagger a | \mathcal{E}_0 \rangle$ in the uncoupled eigenstates $|\mathcal{E}_0\rangle$ are small compared to N, $\xi \ll N$ and $\chi \ll N$. We now calculate $\mathcal{E}$ by dropping all $s + s' \geq 2$ terms and show that for the low-energy spectrum of $\mathcal{H}_{\mathrm{mic}}$ all matrix elements that induce transitions in-between excited atomic states are irrelevant. To that end, we write

$$\mathcal{H}_{\mathrm{mic}} = \tilde{\omega} a^\dagger a + \sum_{k=1}^{N} \sum_{l,l'=0}^{\mu} \left(\Omega_l \delta_{l,l'} |l_k\rangle\langle l_k| + i A_0 \sqrt{\frac{\tilde{\omega}}{\omega}} (\Omega_{l'} - \Omega_l) d_{l,l'} (a^\dagger + a) |l_k\rangle\langle l'_k| \right) + C, \tag{S21}$$

with $\tilde{\omega} = \sqrt{\omega^2 + 4\kappa\omega}$ and $C = (\tilde{\omega} - \omega)/2$, and we define

$$H = \tilde{\omega}a^\dagger a + \sum_{k=1}^{N}\sum_{l=1}^{\mu}\Omega_l|l_k\rangle\langle l_k| \tag{S22a}$$

$$H_{\mathrm{cpl}} = (a^\dagger + a)\sum_{k=1}^{N}\sum_{l=1}^{\mu}A_0\sqrt{\frac{\tilde{\omega}}{\omega}}\Omega_l\big(id_{0,l}|0_k\rangle\langle l_k| - id_{l,0}|l_k\rangle\langle 0_k|\big) \tag{S22b}$$

$$\Delta H = (a^\dagger + a)\sum_{k=1}^{N}\sum_{l>l'\geq 1}^{\mu}A_0\sqrt{\frac{\tilde{\omega}}{\omega}}(\Omega_l - \Omega_{l'})\big(id_{l',l}|l'_k\rangle\langle l_k| - id_{l,l'}|l_k\rangle\langle l'_k|\big). \tag{S22c}$$

Accordingly,

$$\mathcal{E} \propto \langle\mathcal{E}|\mathcal{H}_{\mathrm{mic}}|\mathcal{E}\rangle \tag{S23a}$$

$$\propto \langle\mathcal{E}_0|H|\mathcal{E}_0\rangle + A_0\big(\langle\mathcal{E}_0|H_{\mathrm{cpl}}|\mathcal{E}_1\rangle + \langle\mathcal{E}_1|H_{\mathrm{cpl}}|\mathcal{E}_0\rangle + \langle\mathcal{E}_0|\Delta H|\mathcal{E}_1\rangle + \langle\mathcal{E}_1|\Delta H|\mathcal{E}_0\rangle\big). \tag{S23b}$$

Let us now compare the contributions of H_{cpl} and ΔH to $\mathcal{E}$. The photonic parts of H_{cpl} and ΔH are equal and need not be further considered. We write $\langle H_{\mathrm{cpl}}\rangle = \langle\mathcal{E}_0|H_{\mathrm{cpl}}|\mathcal{E}_1\rangle + \langle\mathcal{E}_1|H_{\mathrm{cpl}}|\mathcal{E}_0\rangle$ and $\langle\Delta H\rangle = \langle\mathcal{E}_0|\Delta H|\mathcal{E}_1\rangle + \langle\mathcal{E}_1|\Delta H|\mathcal{E}_0\rangle$, and we find

$$\frac{\langle\Delta H\rangle}{\langle H_{\mathrm{cpl}}\rangle} = \frac{\sum_{l>l'\geq 1}^{\mu}(\Omega_l - \Omega_{l'})\mathrm{Im}\big[d_{l',l}\sum_{k=1}^{N}\big(\langle\mathcal{E}_0|l'_k\rangle\langle l_k|\mathcal{E}_1\rangle + \langle\mathcal{E}_1|l'_k\rangle\langle l_k|\mathcal{E}_0\rangle\big)\big]}{\sum_{l=1}^{\mu}\Omega_l\mathrm{Im}\big[d_{0,l}\sum_{k=1}^{N}\big(\langle\mathcal{E}_0|0_k\rangle\langle l_k|\mathcal{E}_1\rangle + \langle\mathcal{E}_1|0_k\rangle\langle l_k|\mathcal{E}_0\rangle\big)\big]} \tag{S24}$$

Since $N \to \infty$, the number of nonzero terms in the k-sums is decisive. For given l, l', the sum over k in the numerator has at most ξ nonzero terms, whereas the sum over k in the denominator has at least $N - \xi$ nonzero terms. Hence, we drop ΔH, which represents the matrix elements of $\mathcal{H}_{\mathrm{mic}}$ connecting the excited states of an atom, and keep H_{cpl} as the relevant coupling part of $\mathcal{H}_{\mathrm{mic}}$. We reintroduce the κ-term and call the resulting Hamiltonian *generalized Dicke Hamiltonian* $\mathcal{H}_{\mathrm{GD}}$,

$$\mathcal{H}_{\mathrm{GD}} = \omega a^\dagger a + \kappa(a^\dagger + a)^2 + \sum_{k=1}^{N}\sum_{l=1}^{\mu}\big(\Omega_l|l_k\rangle\langle l_k| - \Omega_l A_0(a^\dagger + a)\big(id_{l,0}|l_k\rangle\langle 0_k| + \mathrm{H.c.}\big)\big). \tag{S25}$$

It has the same low-energy spectrum as $\mathcal{H}_{\mathrm{mic}}$. Paralleling our treatment of $\mathcal{H}_{\mathrm{D}}$, we introduce

$$a_{k,l}^\dagger = |l_k\rangle\langle 0_k|, \qquad b_{q_j,l}^\dagger = \frac{1}{\sqrt{N}}\sum_{k=1}^{N}e^{iq_j k}|l_k\rangle\langle 0_k|, \tag{S26}$$

where $q_j = 2\pi(j/N)$ and $j \in \{0, 1, \ldots, N-1\}$ as before. With $\sum_{k=1}^{N}a_{k,l}^\dagger a_{k,l} = \sum_{j=0}^{N-1}b_{q_j,l}^\dagger b_{q_j,l}$, Eq. (S25) becomes

$$\mathcal{H}_{\mathrm{GD}} = \omega a^\dagger a + \kappa(a^\dagger + a)^2 + \sum_{l=1}^{\mu}\Big(\Omega_l\sum_{j=0}^{N-1}b_{q_j,l}^\dagger b_{q_j,l} - A_0\Omega_l\sqrt{N}(a^\dagger + a)\big(id_{l,0}b_{q_0,l}^\dagger + \mathrm{H.c.}\big)\Big). \tag{S27}$$

The operators $b_{q_j,l}$ are bosonic in the limit of dilute excitations ($\xi \ll N$)[3]. The $j > 0$ collective modes do not couple to the electromagnetic field. Again, we drop the energy of

these 'dark' modes, write b_l instead of $b_{q_0,l}$, define $\lambda = A_0 \Omega_l |d_{0l}| \sqrt{N}$, and remove the κ-term by substituting $\omega \to \tilde{\omega} = \sqrt{\omega^2 + 4\kappa\omega}$ and $\lambda_l \to \tilde{\lambda}_l = \sqrt{\omega/\tilde{\omega}}\lambda_l$ and adding $C = (\tilde{\omega} - \omega)/2$. This gives

$$\mathcal{H}_{\mathrm{GD}} = \tilde{\omega}a^\dagger a + \sum_{l=1}^{\mu} \Omega_l b_l^\dagger b_l + \sum_{l=1}^{\mu} \tilde{\lambda}_l(b_l^\dagger + b_l)(a^\dagger + a) + C. \tag{S28}$$

In order to find the eigenfrequencies of $\mathcal{H}_{\mathrm{GD}}$, we introduce canonical coordinates by means of

$$x = \frac{1}{\sqrt{2\tilde{\omega}}}(a^\dagger + a), \quad p_x = i\sqrt{\frac{\tilde{\omega}}{2}}(a^\dagger - a), \quad y_l = \frac{1}{\sqrt{2\Omega_l}}(b_l^\dagger + b_l), \quad p_l = i\sqrt{\frac{\Omega_l}{2}}(b_l^\dagger - b_l), \tag{S29}$$

and define $\mathbf{X}^{\mathrm{T}} = (x, y_1, \ldots, y_\mu)$, $\mathbf{P}^{\mathrm{T}} = (p_x, p_1, \ldots, p_\mu)$, and $g_l = 2\tilde{\lambda}_l\sqrt{\tilde{\omega}\Omega_l}$. This yields

$$\mathcal{H}_{\mathrm{GD}} = \frac{\mathbf{P}^{\mathrm{T}}\mathbf{P}}{2} + \frac{1}{2}\mathbf{X}^{\mathrm{T}}\underline{\Omega}^2\mathbf{X} - \frac{1}{2}\Big(\omega + \sum_{l=1}^{\mu} \Omega_l\Big) \tag{S30}$$

where

$$\underline{\Omega}^2 = \begin{pmatrix} \tilde{\omega}^2 & g_1 & \cdots & g_\mu \\ g_1 & \Omega_1^2 & & \\ \vdots & & \ddots & \\ g_\mu & & & \Omega_\mu^2 \end{pmatrix} \tag{S31}$$

The orthogonal matrix G that diagonalizes $\underline{\Omega}^2$ induces a point transformation to the normal modes $\tilde{\mathbf{X}} = G\mathbf{X}$ and $\tilde{\mathbf{P}} = G\mathbf{P}$. The eigenvalues ϵ_i^2 of $\underline{\Omega}^2$ are the squared eigenfrequencies of the system. They solve the characteristic equation

$$0 = \Big(\prod_{l'=1}^{\mu} (\Omega_{l'}^2 - \epsilon^2)\Big)\Big((\tilde{\omega}^2 - \epsilon^2) - \sum_{l=1}^{\mu} \frac{g_l^2}{\Omega_l^2 - \epsilon^2}\Big) \tag{S32a}$$

$$= \Big(\prod_{l'=1}^{\mu} (\Omega_{l'}^2 - \epsilon^2)\Big)\Big((\tilde{\omega}^2 - \epsilon^2) - 4\tilde{\omega}\sum_{l=1}^{\mu} \frac{\Omega_l \tilde{\lambda}_l^2}{\Omega_l^2 - \epsilon^2}\Big). \tag{S32b}$$

None of them can be zero since this would imply

$$\frac{\omega}{4NA_0^2} = \sum_{l=1}^{\mu} \Omega_l |d_{0l}|^2 - \sum_{i=1}^{n} \frac{q_i^2}{2m_i}. \tag{S33}$$

We have used $\tilde{\omega} = \sqrt{\omega^2 + 4\kappa\omega}$, $\tilde{\lambda}_l = \sqrt{\omega/\tilde{\omega}}\lambda_l$, $\lambda_l = A_0 \Omega_l |d_{0l}| \sqrt{N}$, and $\kappa = NA_0^2 \sum_{i=1}^{n} q_i^2/2m_i$. However, the left side of Eq. (S33) is positive, whereas its right side is negative according to the TRK for H_{mic}^0 (Eqs. (S3) or Eq. (9) of the main text).

E. Influence of disorder in the atomic parameters. The unavoidable fluctuations of the transition frequencies and coupling strengths of the artificial atoms may be expected to weaken the tendency towards a SPT in a circuit QED system and thus should not jeopardize the assertion of the no-go theorem. However, the experimental verification of the failure of the standard description of circuit QED proposed in the main text requires that the coupling-induced shift of the resonator frequency and the SPT predicted by the standard description are robust with respect to some disorder in the atomic parameters. Further, for a coupling that is critical according to the standard description, the minimal excitation energy compatible with the TRK has to be well-separated form zero also for a disordered system.

In this section, we present numerical results showing that disorder in the atomic parameters does not have a significant influence on the lowest excitation energy of a circuit QED system with a large number of artificial atoms, both according to the standard description of circuit QED and according to a microscopic description that obeys the TRK. The proposed method for experimentally observing the failure of the standard description is consequently not affected by a small amount of disorder in the atomic parameters. Finally, we show that in case of very strong coupling, the failure of the standard description of circuit QED can become measurable already for a system with $N = 10$.

Neither in the standard description nor in the microscopic description it is possible to numerically calculate the excitation energies for a system containing as many as $N \sim 200$ artificial atoms. One can therefore not demonstrate in this way that also for disordered systems the standard description predicts a SPT, whereas according to the microscopic description all excitation energies remain nonzero. Hence, we will follow a strategy pursued in a similar context in Ref. [4] and consider smaller systems with varying number of artificial atoms to study the effect of disorder under increasing system size. For non-identical artificial atoms, the Dicke Hamiltonian reads

$$\mathcal{H}_{\mathrm{D}} = \omega a^{\dagger} a + \sum_{k=1}^{N} \frac{\Omega_k}{2} \sigma_z^k + \sum_{k=1}^{N} \frac{\lambda_k}{\sqrt{N}} \sigma_x^k (a^{\dagger} + a) + \sum_{k=1}^{N} \kappa_k (a^{\dagger} + a)^2, \tag{S34}$$

where κ_k represents the $\mathbf{A}^2$-terms due to a single atom ($\kappa = \sum_{k=1}^{N} \kappa_k$). Note that Ω_k, λ_k, and κ_k depend on the properties of the kth atom and may slightly fluctuate in a way that has to be specified. The effective model for an artificial atom employed in the standard description leads to (cf. Eqs. (5) of the main text)

$$\lambda_{\mathrm{cir},k} = \frac{eC_{\mathrm{G}}^k}{C_{\mathrm{G}}^k + C_{\mathrm{J}}^k} \sqrt{\frac{\omega N}{Lc}}, \qquad \kappa_{\mathrm{cir},k} = \frac{(C_{\mathrm{G}}^k)^2}{2(C_{\mathrm{G}}^k + C_{\mathrm{J}}^k)} \frac{\omega}{Lc}, \tag{S35}$$

while the microscopic approach yields (cf. Eqs. (8) of the main text)

$$\lambda_{\mathrm{cir},k}^{\mathrm{mic}} = \frac{\Omega_k |\boldsymbol{\epsilon} \cdot \mathbf{d}^k|}{\sqrt{2\epsilon_0 \omega}} \sqrt{\frac{N}{V}}, \qquad \kappa_{\mathrm{cir},k}^{\mathrm{mic}} = \frac{1}{2\epsilon_0 \omega V} \sum_{i=1}^{n_k} \frac{(q_i^k)^2}{2m_i^k}, \tag{S36}$$

and $\mathbf{d}^k = \langle \mathrm{e}_k | \sum_{i=1}^{n_k} q_i^k \mathbf{r}_i^k | \mathrm{g}_k \rangle$. We define a parameter α_k via $N\kappa_k = \alpha_k \lambda_k^2 / \Omega_k$ and find

$$\alpha_{\mathrm{cir},k} = \frac{E_{\mathrm{J}}^k (C_{\mathrm{G}}^k + C_{\mathrm{J}}^k)}{2e^2} \equiv \frac{E_{\mathrm{J}}^k}{4E_{\mathrm{C}}^k}, \qquad \alpha_{\mathrm{cir},k}^{\mathrm{mic}} = \frac{\sum_{i=1}^{n_k} (q_i^k)^2 / 2m_i^k}{\Omega_k |\boldsymbol{\epsilon} \cdot \mathbf{d}^k|^2}, \tag{S37}$$

where $\alpha_{\mathrm{cir},k}^{\mathrm{mic}} \geq 1$ due to the TRK (Eq. (9) of the main text). We assume for the microscopic description $\alpha_{\mathrm{cir},k}^{\mathrm{mic}} = 1$, which corresponds to the strongest shift of the lowest excitation energy

allowed by the TRK (in other words, the atoms are taken to be perfect two-level systems). Now we implement disorder in the system and write $\Omega_k = \Omega \tau_k$, where we choose τ_k to be a random number following a normal distribution with mean 1 and standard deviation 0.1. To determine how disorder in the Ω_k affects λ_k and κ_k both in the standard and in the microscopic description of the system, it is further assumed that the artificial atoms have approximately the same shape and chemical composition, that the disorder is only due to imperfections in the fabrication of the Josephson junctions, and that $C_G \gg C_J^k$. Thus, $\kappa_{\text{cir},k} = \kappa_{\text{cir}}/N$ and $\kappa_{\text{cir},k}^{\text{mic}} = \kappa_{\text{cir}}^{\text{mic}}/N$ are taken to be independent of k. Under these conditions, $\lambda_{\text{cir},k}^{\text{mic}} = \lambda_{\text{cir}}^{\text{mic}} \sqrt{\tau_k}$, whereas $\lambda_{\text{cir},k} = \lambda_{\text{cir}}$ does not depend on the fluctuations of the atomic transition frequencies. Note that $\alpha_{\text{cir},k} = E_{\text{J},k}/4E_\text{C} = \Omega_k/4E_\text{C} = (E_\text{J}/4E_\text{C})\tau_k = \alpha_{\text{cir}}\tau_k$. By fixing $\alpha_{\text{cir}} = E_\text{J}/4E_\text{C} = 0.1$ as in the calculation for the ordered system, we have expressed Ω_k, λ_k and κ_k both in the standard and in the microscopic description of the disordered system by mean values Ω and λ and a disorder configuration $\{\tau_k\}$.

In our numerical analysis, we calculate the lowest excitation energies $\epsilon_-^{N,\text{d}}$ of disordered circuit QED systems with $N = 3, 5, 7$ artificial atoms as functions of λ according to the standard and the microscopic description. It will be necessary to consider couplings of the same order of magnitude as Ω. Even though with present-day technologies such couplings are not realistic for $N = 3, 5, 7$, this gives us the evolution of the lowest excitation energy with increasing N under strong coupling and allows us to infer the behavior of a system with larger N, for which $\lambda \sim \Omega$ is possible ($\lambda \propto \sqrt{N}$), but which would be numerically intractable. All calculations are done for $\omega = \Omega$, and we have used 100 disorder configurations for each system size to calculate mean values $\langle \epsilon_-^{N,\text{d}} \rangle$ and standard deviations σ_N. Numerical experiments show that restricting the photonic part of the Hilbert space to maximally seven photons provides a good compromise between accuracy and numerical effort. We have also calculated the lowest excitation energies ϵ_-^N of the corresponding ordered systems ($\tau_k = 1$ for all k), and we compare our results with ϵ_-^∞ (for different α), the exact lowest excitation energy of an infinitely large ordered system (Eq. (7) and Fig. 2(a) of the main text, there denoted simply by ϵ_-).

Figure S2 shows our main numerical results. We plot in black the excitation energies of the homogeneous systems, ϵ_-^N, for $N = 3, 5, 7$. The upper three black curves are calculated according to the microscopic description of circuit QED, the lower ones according to the standard description of circuit QED. In both cases, the frequency shift for given λ increases with N. For comparison, we plot the corresponding analytically found excitation energies for the infinitely large homogeneous system, $\epsilon_-^\infty|_{\alpha=0.1}$ (dark red) and $\epsilon_-^\infty|_{\alpha=1}$ (dark green). The latter curve already appeared in Fig. 2(a) of the main text. Indeed, as N increases, ϵ_-^N approaches $\epsilon_-^\infty|_{\alpha=0.1}$ (or $\epsilon_-^\infty|_{\alpha=1}$) if calculated according to the standard (or microscopic) description of circuit QED.

We plot further the averaged lowest excitation energies $\langle \epsilon_-^{N,\text{d}} \rangle$ (dashed blue, dashed green, and dashed magenta for $N = 3, 5, 7$, respectively), again both according to the microscopic description (upper three curves) and according to the standard description (lower three curves). The figure clearly demonstrates that the mean excitation energies of the disordered systems are similar to the excitation energies of the homogeneous systems. The dashed lines for $\langle \epsilon_-^{N,\text{d}} \rangle$ gained from the standard description are hardly visible for $\lambda/\Omega \gtrsim 0.5$ as they coincide in the resolution of Fig. S2 with the corresponding ϵ_-^N-lines and are plotted underneath.

The solid colored curves enclosing the color-shaded regions represent $\langle \epsilon_-^{N,\text{d}} \rangle \pm \sigma_N$ as calculated from the microscopic and the standard description of circuit QED. We use again blue, green, and magenta for $N = 3, 5, 7$, respectively.

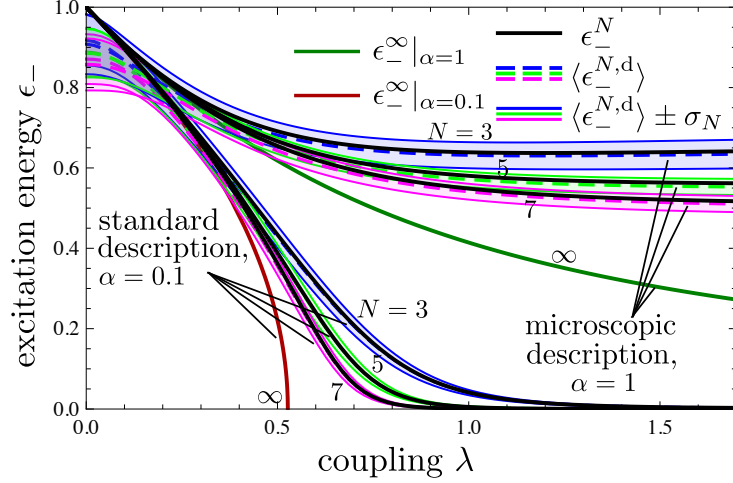According to the microscopic description, the standard deviation does not appreciably

Figure S2: Lowest excitation energies of (dis-)ordered circuit QED systems with varying number of artificial atoms vs. coupling λ. The figure shows the predictions both of the standard description of circuit QED and of a microscopic description that is compatible with the Thomas-Reiche-Kuhn sum rule. Scales are in units of $\omega = \Omega$. Black lines: lowest excitation energies of ordered circuit QED systems with $N = 3, 5, 7$ artificial atoms according to the microscopic description (upper three curves) and according to the standard description (lower three curves). Blue, green, and magenta lines: results for the corresponding disordered systems. Mean excitation energies are represented by dashed lines, while the solid lines stand for the mean values plus and minus the standard deviation. Furthermore, analytical results for a homogeneous system with $N \to \infty$ according to the standard description (dark red) and according to the microscopic description (dark green). The standard description predicts precursors of the superradiant phase transition for the disordered finite-size systems. For couplings that produce a quasi-degenerate ground state according to the standard description, the microscopic description predicts a nonzero energy gap, irrespective of the presence of disorder in the atomic parameters.

decrease with increasing λ. However, the standard deviation is small compared to the mean lowest excitation energy $\langle \epsilon_-^{N,\mathrm{d}} \rangle$ and decreases with N, $\sigma_3 > \sigma_5 > \sigma_7$ for all λ. Disorder, thus, does not have a significant effect on the lowest excitation energy of a circuit QED system containing many artificial atoms according to the microscopic description. The lower bound derived in the main text for the shifted resonator frequency of a homogeneous circuit QED system undergoing a SPT according to the standard description will basically remain unchanged if a small amount of disorder in the atomic parameters is admitted.

According to the standard description, the effect of disorder is strongly suppressed for large λ. The lowest excitation energies of the disordered systems do not only coincide on average with the excitation energies of the homogeneous systems, also the standard deviation from the mean rapidly shrinks with λ and N. For instance, for $N = 7$ and $\lambda/\Omega = 1.5$, we find by means of the standard description $\epsilon_-^7/\Omega \approx 10^{-5}$, $\langle \epsilon_-^{7,\mathrm{d}} \rangle/\Omega \approx 10^{-5}$, and $\sigma_7/\Omega \approx 2 \times 10^{-6}$. This means that the ground states of the systems become quasi-degenerate for strong coupling λ, irrespective of the presence of disorder. Hence, in the standard description of circuit QED precursors of the SPT are visible for finite-size disordered systems and get more pronounced with increasing N. The effect of disorder is much weaker than the coupling-induced frequency

shift and vanishes where the corresponding ordered systems become gapless. Consequently, our estimate on the basis the standard description of how many artificial atoms are required to see signatures of a SPT in a homogeneous circuit QED system with realistic parameters (see main text) will not be affected by small fluctuations of the atomic parameters.

Taken together, our numerical results for the microscopic and the standard description assure – as the central conclusion of this section – that the method for experimentally observing the failure of the standard description of circuit QED systems that we have proposed in the main text is insensitive to a small amount of disorder in the atomic parameters.

We remark that we have done the same analysis of (dis-)ordered finite-size circuit QED systems as above on the basis of the microscopic description but with $\alpha = 0$ (Fig. S3). This shows how the SPT emerges in a (dis-)ordered circuit or cavity QED system according to the microscopic picture if the κ-term is disregarded (recall that the dependence of λ_j on Ω_j differs between standard and microscopic description). One finds very similar results as for the standard description of circuit QED: the mean lowest excitation energies (dashed colored lines) converge to those of the homogeneous systems (black lines) as λ increases, the standard deviation (solid colored lines, plotted relative to the mean values) shrinks even faster than in the standard description, and the (mean) excitation energies approach $\epsilon_-^\infty|_{\alpha=0}$ (red line) if N is increased. The latter curve already appeared in Fig. 2(a) of the main text. These findings imply that if a SPT occurred in a homogeneous system (this happened if $\alpha < 1$
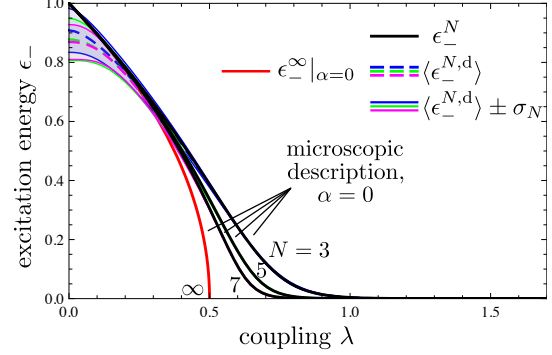

Figure S3: Lowest excitation energies of (dis-)ordered circuit QED systems with varying number of artificial atoms vs. coupling λ (in units of $\omega = \Omega$). The figure shows the predictions the microscopic description if the κ-term is neglected ($\alpha = 0$). The color code is the same as in Fig. S2. Furthermore, the analytical result for a homogeneous system with $N \to \infty$ if the κ-term is neglected (red).

according to Eq. (2)), it would be not affected by some disorder in the atomic parameters, not only according to the standard description but also according to the microscopic description of circuit QED.

Finally, we numerically estimate the deviation of the prediction of the standard description of circuit QED from the actual value for the lowest excitation energy of a circuit QED system with only 10 artificial atoms but with very strong coupling. Suppose an artificial atom couples with a strength $\lambda/\Omega = 0.1$ to the resonator field. This has been already achieved with flux qubits [5] and is referred to as "ultrastrong coupling". Since we have seen that disorder plays only a minor role for the lowest excitation energy of a circuit QED systems with $N \gg 1$, we consider for simplicity a homogeneous system. We assume again $\omega = \Omega$, include up to 10 photons in our calculations, and obtain, by taking the $\sqrt{N}$-scaling of the coupling into account, excitation energies of $\epsilon_-^{10}|_{\alpha=0.1}/\Omega \approx 0.63$ (corresponding to the standard description with $\alpha_{\mathrm{cir}} = E_J/4E_C = 0.1$, cf. Eqs. (S37)) and $\epsilon_-^{10}|_{\alpha=1}/\Omega \approx 0.74$ ($\alpha = 1$ corresponds to the strongest frequency shift compatible with the TRK, i.e., to the microscopic description of ideal two-level artificial atoms, cf. Eqs. (S37) and Eq. (9) of the main text). This means that, if the coupling is ultrastrong, already for systems with ~ 10 artificial atoms the standard

description can be measurably inaccurate: in the case considered here, the actually measured lowest excitation energy will be at least 17% greater than predicted by the standard description. Measuring the excitation energy of such a system hence could be an alternative viable way to experimentally verify our conclusions. Ultimately, these deliberations may give an improved idea of the required system sizes and coupling strengths that render the mistakes made by the standard description manifest.

References

[1] W. Thomas, Naturwissenschaften **13**, 627 (1925); F. Reiche and W. Thomas, Z. Phys. **34**, 510 (1925); W. Kuhn, *ibid.* **33**, 408 (1925).

[2] C. Emary and T. Brandes, Phys. Rev. Lett. **90**, 044101 (2003); C. Emary and T. Brandes, Phys. Rev. E **67**, 066203 (2003).

[3] J. J. Hopfield, Phys. Rev. **112**, 1555 (1958).

[4] P. Nataf and C. Ciuti, Phys. Rev. Lett. **104**, 023601 (2010).

[5] T. Niemczyk *et al.*, Nature Phys. **6**, 772 (2010).